

Influence of the Péclet number on reactive viscous fingering

Priyanka Shukla^{1,*} and A. De Wit^{2,†}¹*Department of Mathematics, Indian Institute of Technology Madras, Chennai 600036, India*²*Université libre de Bruxelles (ULB), Nonlinear Physical Chemistry Unit, CP231, Faculté des Sciences, Campus Plaine, 1050 Brussels, Belgium*

(Received 9 February 2018; revised manuscript received 10 August 2019; published 27 January 2020)

The hydrodynamic viscous fingering instability can be influenced by a simple viscosity-changing chemical reaction of type $A + B \rightarrow C$, when a solution of reactant A is injected into a solution of B and a product C of different viscosity is formed by reaction. We investigate here numerically such reactive viscous fingering in the case of a reaction decreasing the viscosity to define the optimal conditions on the chemical and hydrodynamic parameters for controlling fingering. In particular, we analyze the influence of the Péclet number, Pe , on the efficiency of the chemical control of fingering. We show that the viscosity-decreasing reaction has an increased stabilizing effect when Pe is decreased. On the contrary, fingering is more intense and the system more unstable when Pe is increased. The related reactive fingering patterns cover then respectively a smaller (larger) area than in the nonreactive equivalent. Depending on the value of the Péclet number, a given chemical reaction may thus either enhance or suppress a fingering instability. This stabilization and destabilization at low and high Pe are shown to be related to the Pe -dependent characteristics of a minimum in the viscosity profile that develops around the miscible interface thanks to the effect of the chemical reaction.

DOI: [10.1103/PhysRevFluids.5.014004](https://doi.org/10.1103/PhysRevFluids.5.014004)

I. INTRODUCTION

A hydrodynamic viscous fingering (VF) instability can deform the interface between two different fluids when a high mobility fluid of lower viscosity displaces a more viscous and hence less mobile one in a porous medium [1–5]. In numerous industrial and environmental problems, such as enhanced oil recovery (EOR), CO₂ sequestration, combustion, hydrology, and soil remediation, to name a few [6–10], this fingering instability can interplay with chemical reactions. In the past few decades, viscous fingering has been analyzed in reactive systems on both miscible and immiscible interfaces [11–37]. If the reaction does not modify the viscosity *in situ*, the chemical species are passively advected by the flow and the fingering properties of the interface remain similar to those of the nonreactive system [11–15]. The flow in the fingering patterns can, however, change the spatiotemporal distribution of the reactants and influence the yield of the reaction. The active influence of chemistry on fingering can be obtained as soon as the chemical reaction taking place around the interface between the two fluids modifies their physical properties and, in particular, their viscosity [35–37]. The reaction then influences the stability as well as the spatiotemporal dynamics of the flow. In turn, the hydrodynamic flow affects mixing and thus the amount and spatial distribution of chemical species and a highly nonlinear feedback is established between chemistry and hydrodynamics.

*priyanka@iitm.ac.in

†adewit@ulb.ac.be

For cases where reactions actively change the viscosity *in situ*, numerical simulations have first shown on the basis of a bistable chemical reaction scheme that the properties of miscible VF are modified when the reaction changes the viscosity across the reactive miscible interface [16,17]. The bistable nature of chemical kinetics is then responsible for a new phenomenon of droplet formation isolating regions of high or low viscosity within connected domains of the other steady state. In other studies, the active influence of $A + B \rightarrow C$ types of chemical reactions on miscible VF has been studied both experimentally [19,20,22,27–29,31–33] and theoretically [21,23–26,28,30,34]. Various fingering regimes have been identified depending on concentrations, fluid characteristics, and injection flow rate.

In some experiments by Nagatsu *et al.*, a less viscous acidic or basic aqueous solution was injected into a more viscous polymeric solution, the viscosity of which depends on pH [20,22,27]. It is observed that, when the viscosity is increased (decreased) by the reaction, fingers are widened (narrowed), which is mainly due to suppressed (enhanced) shielding effects. Interestingly, opposite results have been observed at moderate reaction rates for systems with a viscosity decrease [22] and increase [27]. In the case where the nonreactive displacement is stable (a more viscous solution displacing a less viscous one), it has even been shown both experimentally and numerically that the reaction is able to trigger VF [28]. Depending whether the reaction increases or decreases viscosity, a different fingering pattern is then obtained.

The experimental study of Nagatsu *et al.* [20] showed that at larger injection rates Q , an instantaneous chemical reaction can have opposite effects on miscible VF when a less viscous (acidic or basic) solution is injected radially into a more viscous one (e.g., polymeric solution) in a Hele-Shaw cell depending whether the reaction locally increases or decreases the viscosity. In the viscosity-increase case, the VF pattern is “denser” in the sense that it covers a more compact area in the Hele-Shaw cell than the nonreactive pattern. On the contrary, a VF pattern covering a smaller area (also qualified as a “less dense pattern”) was reported in the viscosity-decrease reactive case. Recently, new experiments have been carried out focusing on the influence of the injection rate Q on viscosity increasing and decreasing reactive systems [29,38]. Interestingly, it was found that, at lower injection rates, the trends are opposite than at large Q ; i.e., for viscosity-decreasing reactions, the system can be stabilized at low injection flow rates. These experiments [20,29,38] thus clearly show that, in the presence of a viscosity decreasing reaction, the reactive VF patterns can be controlled by varying the flow rate. Moreover, when the reaction-induced viscosity decrease is large enough, a suppression of the VF instability can be obtained at small enough Q . In practice, a change in the flow rate modifies the Péclet number (Pe) of the problem, i.e., the ratio between the diffusive and convective time scales. Even though the effect of varying the relative contribution of advection and diffusion on nonreactive miscible VF has been the focus of recent studies [39,40], the influence of varying the Péclet number has, however, not been addressed theoretically explicitly in the reactive cases.

In this context, our objective is to analyze numerically the influence on the VF instability of changes in the Péclet number, Pe , when a simple $A + B \rightarrow C$ chemical reaction decreases the viscosity *in situ*. To this end, we integrate numerically the reaction-diffusion-convection (RDC) equations of reactive VF in porous media and analyze the properties of the fingering patterns for different values of Pe . We show that a viscosity-decreasing reaction enhances stabilization or destabilization of the interface at respectively low and high Pe , with regard to the nonreactive system. This is related to the possibility for chemistry to build up at low Pe a minimum in the viscosity profile that blocks the further progression of fingering and stabilizes the system. On the contrary, at high Pe , chemistry does not have time to act to decrease the viscosity and the classical enhancement when Pe is increased is then observed.

These results highlight the optimum flow conditions to obtain stabilization by reactions of VF. This is of practical importance as it paves the way to possible chemical control of fingering instabilities appearing in many practical situations ranging from geophysical to environmental problems.

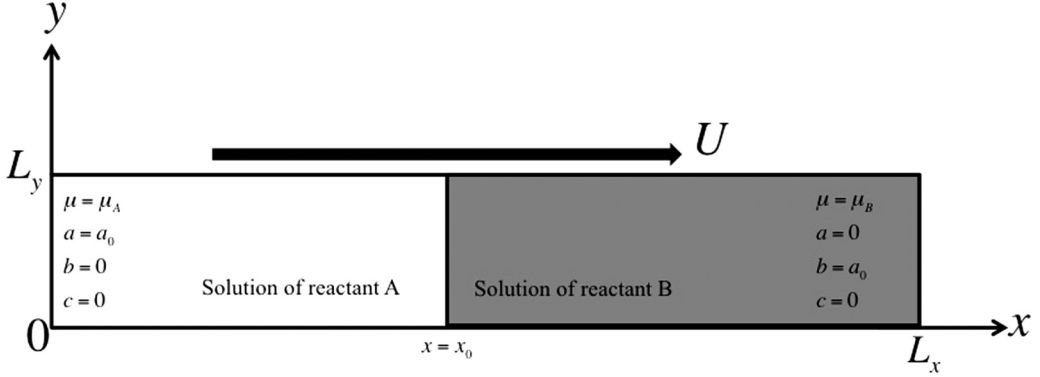


FIG. 1. Sketch of a two-dimensional porous medium of length L_x and width L_y with permeability κ in which a solution of reactant A with viscosity μ_A is displacing a solution of reactant B of viscosity μ_B from left to right at a constant speed U . Here x_0 and a_0 are the initial contact position and initial concentration of reactants, respectively.

This paper is organized as follows. The problem description and the related RDC model are given in Sec. II. In Sec. II C, the numerical method used to integrate the model is discussed. The characteristics of VF patterns and in particular the influence of the Péclet number are studied in Sec. III. The nonreactive and reactive cases are given in Secs. III A and III B, respectively. A quantitative analysis and parametric study are carried out in Secs. III C and IV. At the end, conclusions and outlook are given in Sec. V.

II. PROBLEM DESCRIPTION AND GOVERNING EQUATIONS

A. Dimensional model

Consider a homogeneous two-dimensional porous medium or horizontal thin Hele-Shaw cell of length L_x and width L_y with constant permeability κ in which a miscible solution of reactant A with viscosity μ_A is injected from left to right into a solution of reactant B with viscosity μ_B at a constant speed U along the x direction (Fig. 1). We assume that the initial concentrations of A and B are both equal to a_0 . The initial position of the miscible interface is x_0 . Upon contact between the two solutions, a simple $A + B \rightarrow C$ chemical reaction takes place in the miscible interface zone where A and B meet by diffusion, react, and yield the product C of lower viscosity μ_C . The objective is to analyze numerically how the dynamic decrease of viscosity driven by the reaction can influence the VF instability and in particular what is the influence of the Péclet number on this effect.

To analyze the problem, the system is considered as incompressible and neutrally buoyant. The dynamics is modeled using Darcy's law for the velocity field along with three RDC equations for the concentrations:

$$\nabla \cdot \mathbf{u} = 0, \quad (1)$$

$$\nabla p = -\frac{\mu(a, b, c)}{\kappa} \mathbf{u}, \quad (2)$$

$$\frac{\partial a}{\partial t} + \mathbf{u} \cdot \nabla a = D_A \nabla^2 a - k a b, \quad (3)$$

$$\frac{\partial b}{\partial t} + \mathbf{u} \cdot \nabla b = D_B \nabla^2 b - k a b, \quad (4)$$

$$\frac{\partial c}{\partial t} + \mathbf{u} \cdot \nabla c = D_C \nabla^2 c + k a b, \quad (5)$$

where a , b , and c denote the concentrations of the reactants A and B and of the product C , respectively; k is the kinetic constant; p is the pressure; D_A , D_B , and D_C are the diffusivities of the reactants A and B and the product C , respectively; $\mathbf{u} = (u, v)$ is the two-dimensional flow velocity; and κ is the constant permeability. The viscosities of the solution when only one species is present in concentration a_0 are defined as μ_A , μ_B , and μ_C , respectively, in the presence of the reactants A or B or of the product C . Following previous theoretical work [3,16,17,21,23–26,29,30,41,44], we assume the viscosity as an exponential function of the concentrations of A , B , and C :

$$\mu(a, b, c) = \mu_A e^{[R_b b + R_c c]/a_0}. \quad (6)$$

This assumption, which is a good approximation for some solutes [42,43], allows to discuss the relative effect of solution viscosities with only two dimensionless parameters: the log-mobility ratios R_b and R_c , defined as

$$R_b = \ln\left(\frac{\mu_B}{\mu_A}\right) \quad \text{and} \quad R_c = \ln\left(\frac{\mu_C}{\mu_A}\right). \quad (7)$$

For the nonreactive VF case or the equivalent specific reactive case when the product C has the same viscosity as the reactant B (i.e., $R_b = R_c$), the system is unstable when the lower viscosity solution of A displaces the more viscous solution of B , i.e., when $\mu_A < \mu_B$ or $R_b > 0$. Let us analyze how this stability is changed when both μ_C and the relative effect of advection and diffusion are varied.

B. Nondimensional equations

To specifically let the Péclet number appear in the dimensionless problem, the reference scales for length, velocity, time, concentration, viscosity, diffusivity, and pressure are taken as L_y , U , L_y/U , a_0 , μ_A , D_C , and $\mu_A U L_y / \kappa$, respectively. For simplicity, equations are written in a reference frame moving with speed U by transforming variables as $\mathbf{x} \rightarrow \mathbf{x} - U t \mathbf{e}_x$ and $\mathbf{u} \rightarrow \mathbf{u} - U \mathbf{e}_x$ with \mathbf{e}_x being the unit vector along the x direction. The dimensionless forms of (1)–(6) can then be written as

$$\nabla \cdot \mathbf{u} = 0, \quad (8)$$

$$\nabla p = -\mu(a, b, c)(\mathbf{u} + \mathbf{e}_x), \quad (9)$$

$$\frac{\partial a}{\partial t} + \mathbf{u} \cdot \nabla a = \delta_a \text{Pe}^{-1} \nabla^2 a - \text{Da} a b, \quad (10)$$

$$\frac{\partial b}{\partial t} + \mathbf{u} \cdot \nabla b = \delta_b \text{Pe}^{-1} \nabla^2 b - \text{Da} a b, \quad (11)$$

$$\frac{\partial c}{\partial t} + \mathbf{u} \cdot \nabla c = \text{Pe}^{-1} \nabla^2 c + \text{Da} a b, \quad (12)$$

$$\mu(a, b, c) = e^{(R_b b + R_c c)}, \quad (13)$$

where $\text{Da} = k a_0 L_y / U = \tau_h / \tau_c$ is the dimensionless Damköhler number defined as the ratio of the hydrodynamic time scale $\tau_h = L_y / U$ to the chemical time scale $\tau_c = 1 / k a_0$. The Péclet number $\text{Pe} = U L_y / D_C = \tau_D / \tau_h$ is the ratio of the diffusive time $\tau_D = L_y^2 / D_C$ and the advective time τ_h while $\delta_a = D_A / D_C$ and $\delta_b = D_B / D_C$ are the diffusion coefficient ratios. The dimensionless width of the domain becomes thus equal to 1 while the dimensionless length is given by the aspect ratio $\mathcal{A} = L_x / L_y$. Taking the curl of the momentum equation and defining the stream function $\psi(x, y)$ as $u = \partial \psi / \partial y$ and $v = -\partial \psi / \partial x$, we get

$$\nabla^2 \psi = R_b(\psi_x b_x + \psi_y b_y + b_y) + R_c(\psi_x c_x + \psi_y c_y + c_y), \quad (14)$$

$$a_t + a_x \psi_y - a_y \psi_x = \delta_a \text{Pe}^{-1} \nabla^2 a - \text{Da} a b, \quad (15)$$

$$b_t + b_x \psi_y - b_y \psi_x = \delta_b \text{Pe}^{-1} \nabla^2 b - \text{Da} a b, \quad (16)$$

$$c_t + c_x \psi_y - c_y \psi_x = \text{Pe}^{-1} \nabla^2 c + \text{Da} a b, \quad (17)$$

where the subscripts x and t represent the respective derivatives. The last term in (15)–(17) corresponds to the reaction rate \mathcal{R} :

$$\mathcal{R}(x, y, t) = Da a(x, y, t)b(x, y, t), \quad (18)$$

which quantifies the importance of the reaction terms in the dynamics.

Comparing the present RDC model (14)–(17) with those previously studied in the literature [5,21,23,26,39], we note that (i) when $Da=0$ we recover the classical model for nonreactive VF similar to the one studied by Tan and Homsy [5,39], (ii) when $Da \neq 0$, $Pe = 1$, and $R_b = 0$ we obtain the model of reactive VF for solutions of A and B of the same viscosity as analyzed numerically by Gérard and De Wit [21], and (iii) when $Da \neq 0$ and $Pe = \delta_a = \delta_b = 1$, we get back to the reactive VF model with A , B , and C of different viscosity but species diffusing all at the same rate as studied by Hejazi *et al.* [23] and Nagatsu and De Wit [26].

In reality, the various chemical species involved typically do not diffuse at the same rate as when the reaction produces or consumes big molecules like polymers or micelles, for instance [19,32,33]. Differential diffusion effects might then play an important role in fingering as shown previously [21,44,45]. A detailed analysis of double diffusive effects coupled to variations of the Péclet number in reactive conditions is, however, outside the scope of this paper and will be developed in future studies. We keep, therefore, $\delta_a = \delta_b = 1$ in the sequel of this article.

Equations (14)–(17) are integrated using periodic boundary conditions in both directions. This is standard for the transverse direction. In the longitudinal direction, we ensure that this does not have any effect on the dynamics by using a large aspect ratio $\mathcal{A} = L_x/L_y$ such that the dynamics of the reactive zone does not confront its periodic extension [5].

The initial conditions for the stream function and product concentration are taken as $\psi(x, y)=0$ and $c(x, y)=0$, for all (x, y) , respectively. For the initial concentrations of the reactant A and B solutions, we use a step front between $a = 1$, $b = 0$ on the left and $b = 1$, $a = 0$ on the right of $x=x_0$ with a random noise of amplitude of order 10^{-2} added in the front to trigger the instability. The dimensionless system size is $\mathcal{A} \times 1$. Equations (14)–(17) together with the initial and boundary conditions form an initial-boundary value problem with six dimensionless control parameters, namely, Pe , R_b , R_c , Da , δ_a , and δ_b . As we have fixed $\delta_a = \delta_b = 1$ to avoid differential diffusion effects, we explore here the role of tuning Pe and the effect of reaction by varying Da and R_c for a given R_b .

C. Numerical method

To solve Eqs. (14)–(17), we use a pseudospectral numerical scheme based on the discrete Fourier transform library FFTW 3.3.4 [5,16,17,21,46]. The numerical domain ($\mathcal{A} \times 1$) has a size (32×1) and is discretized into 4098×128 mesh points such that the spatial step sizes are $dx = dy = 1/128$. A convergence study analyzing the values of dx , dy and dt below which the nonlinear finger dynamics and the averaged value of the mixing lengths do not change any more has fixed the optimum time step of numerical integration as $dt = 10^{-4}$. To validate our code, we have successfully reproduced previous nonlinear simulation results of nonreactive [5,39] and reactive [21,23,26] systems.

III. RESULTS

A. Nonreactive system

It is already known that, in the absence of any reaction effect ($Da = 0$ or $R_b = R_c$ [23,26]), increasing Pe increases the destabilization of the interface by VF when $R_b > 0$ [4,5,39]. As a reference case, this observation is shown in Fig. 2, which illustrates the concentration of reactants A and B for $Pe = 100$ and $Pe = 1000$, respectively, at four different times. As Pe increases, fingering becomes more intense and the wavelength of the pattern decreases as the interface becomes more unstable. It is also observed that, at low Pe , the deformed interface tends to flatten as time

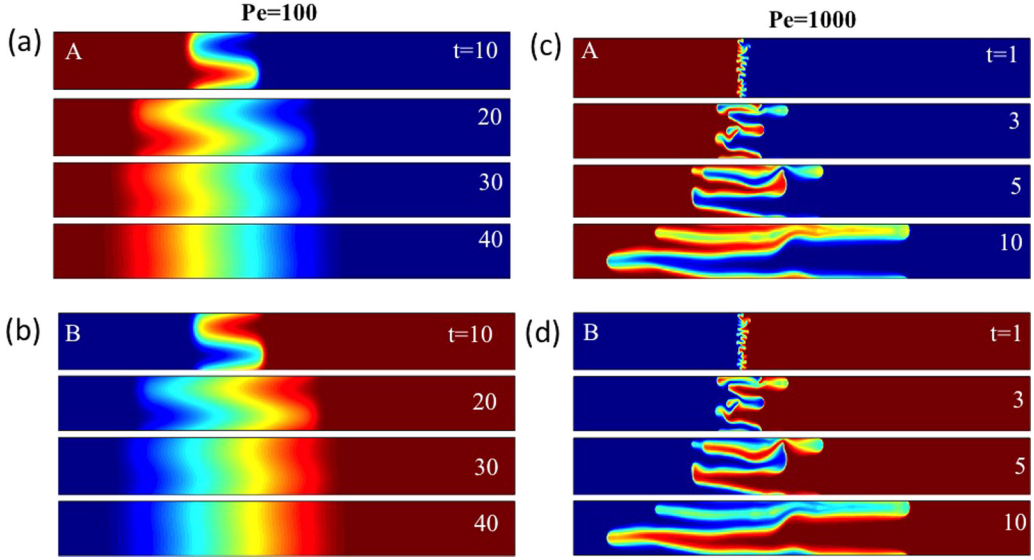


FIG. 2. Equivalent nonreactive ($R_b = R_c = 2$) system: Concentrations of A and B for (a, b) $Pe = 100$ and (c, d) $Pe = 1000$ at four different times (from top to bottom). Concentration fields are scaled between zero (blue) and 1 (red). The viscosity (not shown) varies in a similar way as the concentration of B.

evolves, thanks to transverse diffusion. Note that, as all lengths are scaled here by L_y such that the dimensionless width is equal to 1, the wavelength of the fingers depends in our simulations on Pe . This reference nonreactive case gives more than a dozen fingers at $Pe = 1000$ [Figs. 2(c) and 2(d)].

Figure 3 compares the one-dimensional profiles of the concentrations of A and B, and the logarithm of viscosity, $\ln(\mu)$, at a fixed transverse location $y = L_y/2$ for $Pe = 100$ at $t = 30$ and $Pe = 1000$ at $t = 5$, respectively. As a reference, the white line $y = L_y/2$ is shown in the

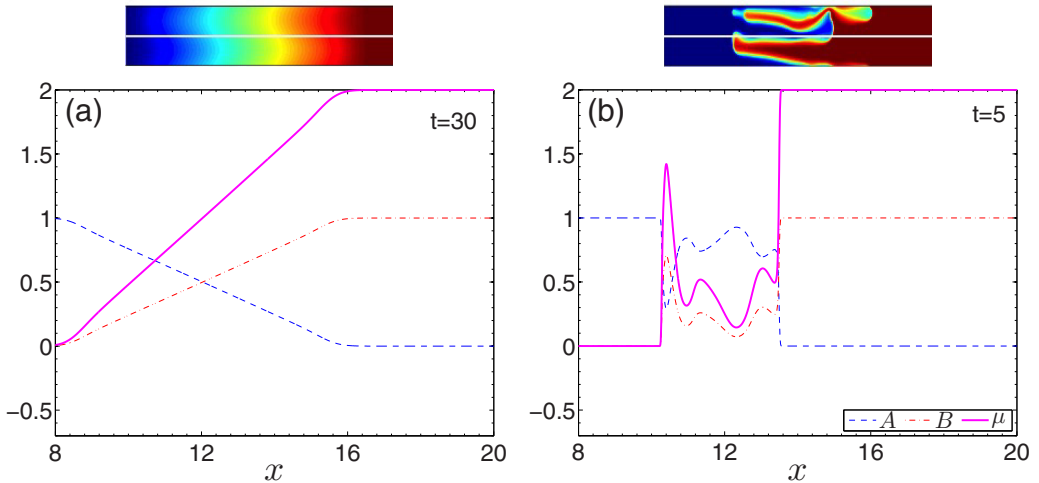


FIG. 3. Spatial profiles of concentrations of A (dashed blue line), B (dash-dotted red line), and of $\ln(\mu)$ (solid magenta line) along the injection direction at $y = L_y/2$ for $R_b = R_c = 2$ and (a) $Pe = 100$ at $t = 30$ and (b) $Pe = 1000$ at $t = 5$ (see Fig. 2). The top figures represent the corresponding two-dimensional map of $\ln(\mu)$ through which the one-dimensional sections are shown.

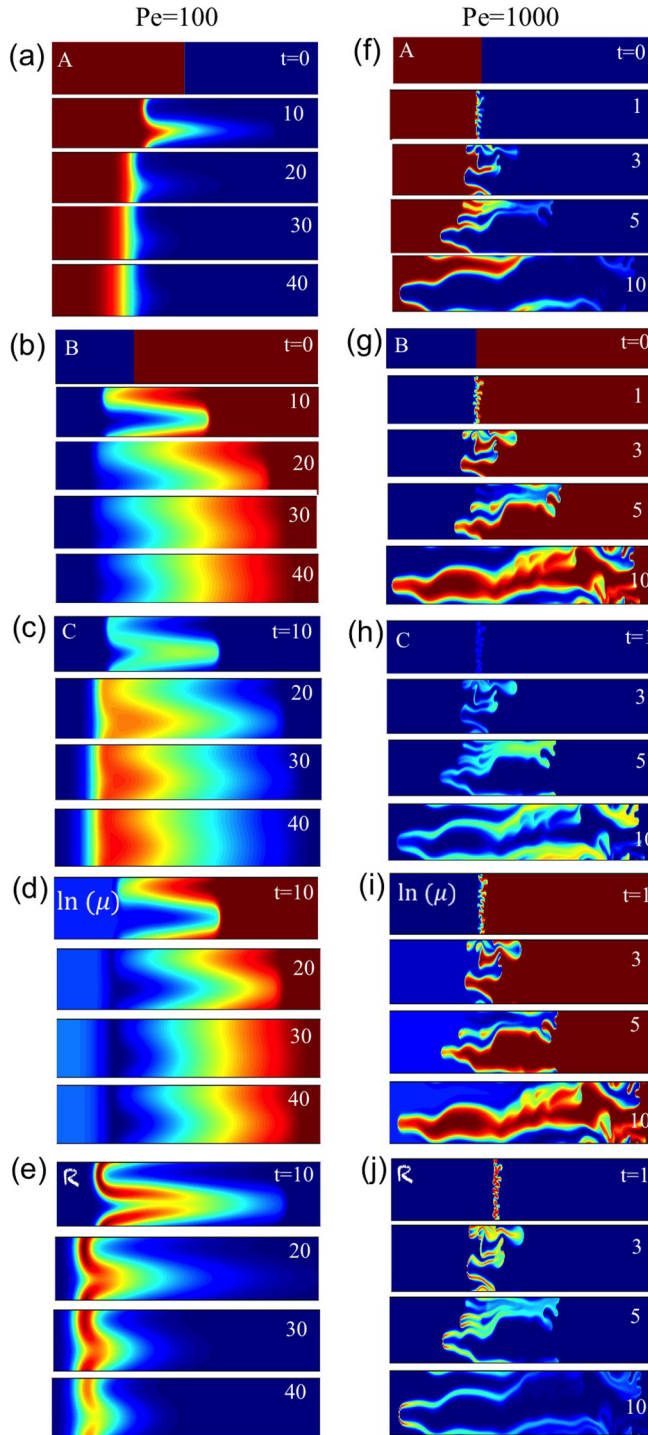
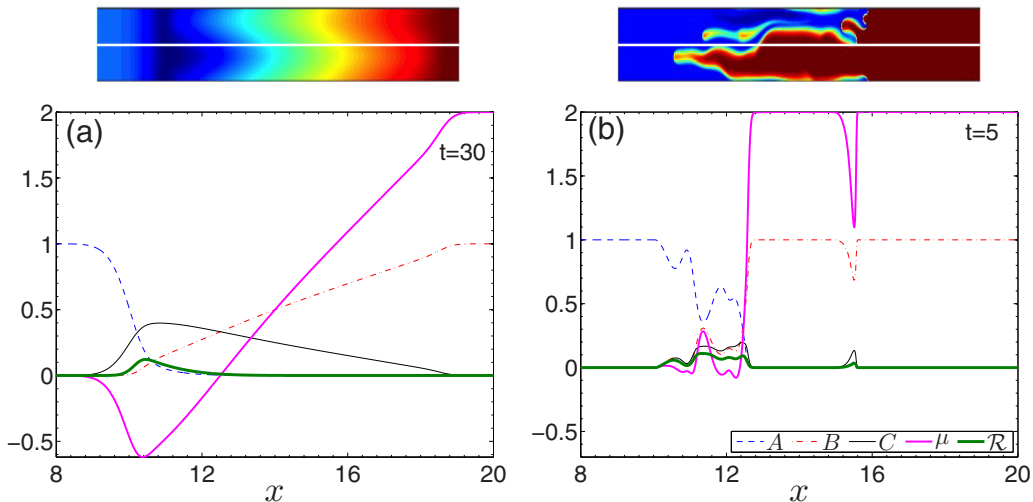


FIG. 4. Reactive VF at $R_b = 2$, $R_c = -2$, and $Da = 1$. The (a–e) first and (f–j) second columns represent the concentrations of A , B , C , viscosity in log-scale $[\ln(\mu)]$, and \mathcal{R} for $Pe = 100$ and 1000 at various times, respectively. A and B are scaled between zero (blue) and 1 (red), C is scaled between zero (blue) and 0.5 (red), and $\ln(\mu)$ and \mathcal{R} are shown in their absolute values.


 FIG. 5. Same as Fig. 3 but for the reactive case at $Da = 1$ (see Fig. 4).

corresponding two-dimensional map of $\ln(\mu)$ on the top of the panels. The concentrations and viscosity profiles at large Pe show bump characteristics of the fingering instability and a sharp jump at the tip of the finger, coherent with an increased destabilization when Pe increases. On the contrary, the profiles are quasilinear between the end-point values at small Pe , indicating a more stable interface. This stabilizing effect at low Pe is in agreement with previous results [3,5,39].

B. Reactive system

Let us now analyze the effect of Pe on reactive VF when an $A + B \rightarrow C$ reaction produces the product C of lower viscosity with a negative value of R_c , such that the viscosity of the system develops in time a minimum around the reactive front.

In order to compare reactive fingering with the nonreactive one of Sec. III A, we consider in this section two representative cases: $Pe = 100$ and $Pe = 1000$. Figure 4 shows the concentrations, $\ln(\mu)$, and reaction rate \mathcal{R} at $Da = 1$, $R_b = 2$, and $R_c = -2$ for $Pe = 100$ and 1000 . Two opposite behaviors are obtained at low and high Pe : At $Pe = 1000$, fingering is more intense than in the nonreactive case with coarsening, and more repetitive shielding and tip splitting [26]. The fingered zone extends on a larger spatial extent than in the nonreactive case (Fig. 2), suggesting that the reaction has here a destabilizing effect. The reaction rate \mathcal{R} [see Eq. (18)], which is nonzero where the reaction proceeds, is seen to extend along the finger edges. Similar to the nonreactive fingering, it is found that the system tends to stabilize for $Pe = 100$. The reaction proceeds essentially in a localized zone at the rear of the finger. As a consequence, more C is produced there which decreases locally the viscosity, stabilizing further the zone between A and C .

A comparison of the one-dimensional profile of the logarithm of the viscosity, $\ln(\mu)$, at location $y = L_y/2$ in the nonreactive [Fig. 3(b)] and reactive [Fig. 5(b)] cases shows that, at $Pe = 1000$, the decrease in viscosity induced by the reaction leads to a sharper viscosity jump which can explain the increased destabilization. As a consequence, fingering extends both in the A - and B -rich regions with the reaction rate being localized at the fingered frontier between the two reactants. On the contrary, at $Pe = 100$, a minimum in viscosity develops in the course of time where the less viscous C is produced by the reaction [Fig. 5(a)]. The reaction rate correspondingly decreases in time and remains strongly localized at a given location [Fig. 4(e)]. The time scales are also longer as more time is needed to cover the same distance. Interestingly, fingering is weak and remains for a longer time in the boundary zone where the less viscous C displaces the more viscous B than in the stable

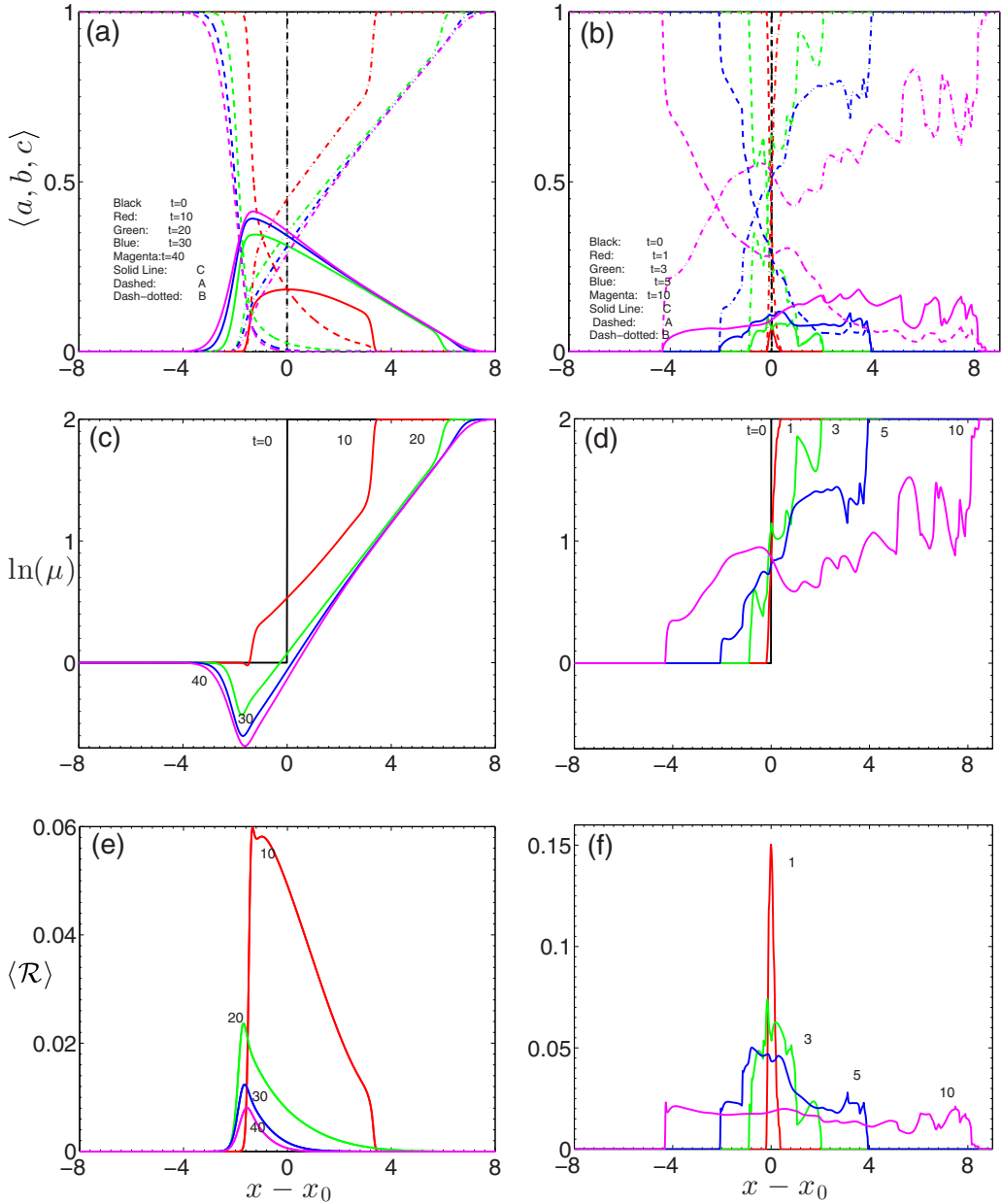


FIG. 6. Transverse averaged (a, b) concentration, (c, d) viscosity, and (e, f) reaction rate profiles corresponding to the reactive fingering case of Fig. 4 for $Pe = 100$ (left column; a, c, e) and $Pe = 1000$ (right column; b, d, f). The dashed, dash-dotted, and solid lines in (a) and (b) depict concentrations of A, B, and C, respectively. The black, red, green, blue, and magenta colors in (a), (c), and (e) correspond to $t = 0, 10, 20, 40$, and 50, respectively, while those in (b), (d), and (f) correspond to $t = 0, 1, 3, 5$, and 10, respectively.

part of the nonmonotonic viscosity profile where A pushes the less viscous C. This means that, in experiments where often a dye is used to visualize the fingering pattern, the instability would quickly become unnoticeable if the dye is diluted in the injected A reactant [29].

A comparison of the spatiotemporal distribution of A in Fig. 2 (nonreactive) and Fig. 4 (reactive) leads thus to the conclusion that, at high Pe , reactive fingering is more intense with more ramified fingers that cover a larger area in the presence of reaction. On the contrary, at low Pe , fingering is stabilized by the reaction. The effect of the reaction decreasing the viscosity has thus an opposite effect on the flow at high and low Pe , as observed experimentally [20,29].

C. Quantitative analysis

In order to understand the opposite dynamics at low and high Pe , and to quantify the influence of varying Pe on reactive VF, we compute the one-dimensional transverse averaged profiles $\langle \zeta \rangle$ of a given quantity $\zeta(x, y, t)$ such as concentration or viscosity, for instance, as

$$\langle \zeta \rangle = \frac{1}{L_y} \int_0^{L_y} \zeta(x, y, t) dy. \quad (19)$$

In the absence of fingering ($R_b = R_c = 0$), these profiles are equivalent to the one-dimensional reaction diffusion profiles. For the simulations of reactive fingering in Fig. 4, the temporal evolution of some of these transversely averaged profiles is shown in Fig. 6.

In the convective flow regime, the fingering pattern starts to develop around the reactive interface as soon as solutions A and B react and produce a less-viscous product C [see Figs. 6(a) and 6(b)]. As the system evolves in time, we see that increasing amounts of A and B are consumed and that the total amount of product $\langle c(x, t) \rangle$ increases. The corresponding reaction rate $\langle \mathcal{R}(x, t) \rangle$, shown in Fig. 6(e), decreases in time when A and B are consumed and are progressively separated by C . Figure 6(c) shows the development of viscosity at low Pe as time evolves. We see that a minimum in viscosity develops in time at the back of the reaction front where the product concentration is maximum which can also be seen from Figs. 4(c) and 4(d). Owing to the viscosity minimum, the interface between A and C is stabilized, which can clearly be observed in Fig. 4(a) as the interface tends to flatten. On the contrary, the interface between B and C where the less viscous C pushes the more viscous B indicates the presence of VF. Nevertheless, transverse diffusion finally dominates VF, and the interface between B and C eventually stabilizes again [see Figs. 4(a)–4(e)].

Let us now analyze quantitatively fingering patterns at larger Pe . We have noticed in Figs. 4(f)–4(j) that reactive VF is destabilizing at high Pe in contrast to a stabilizing trend at low Pe . Figures 6(b), 6(d), and 6(f) show that, at high Pe , when VF is present, the transverse averaged concentration profiles feature bumps, indicating the presence of forward and backward fingering. In contrast to fingering at the back, forward fingering shows merging and tip splitting [see Figs. 4(f)–6(j)]. Similar to the concentration, the log viscosity, Fig. 6(d), and reaction rate profiles, Fig. 6(f), show similar features. The center of mass of these profiles is shifted towards the right of the reaction front, indicating the presence of more elongated fingering in the B -rich region. While, at low Pe , the viscosity minimum formed at the back of the reaction front gives rise to stabilization, it is absent at high Pe because advection dominates the dynamics and does not let the reaction-diffusion processes build up the stabilizing minimum in viscosity. Nevertheless, the gradient in viscosity is sharper, which explains the destabilization at higher Pe .

IV. PARAMETRIC STUDY

We have seen that fingering is stabilized at lower Pe when the viscosity decreases thanks to a chemical reaction. To gain more insight into this stabilization effect, a parametric study is next carried out at several low Pe values to understand the effect of varying the Damköhler number Da and the viscosity of the product by changing the log-mobility ratio R_c .

In order to do so, we compute the mixing lengths L_a , L_b , and L_c of the concentration of reactants A and B and of the product C as the horizontal distance between points where the transverse averaged profile has a value between ϵ and $1 - \epsilon$, where ϵ is a small positive number which is set to 0.01 in

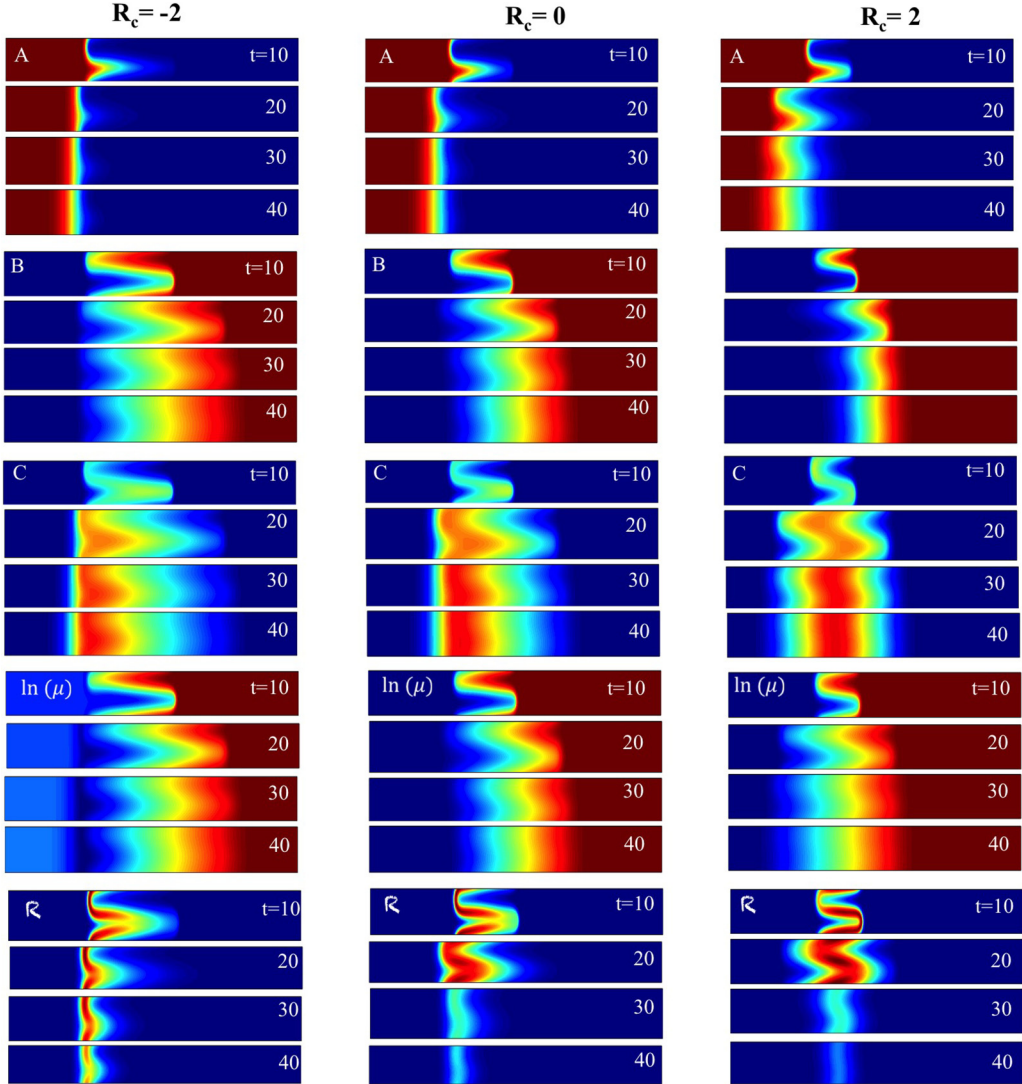


FIG. 7. From top to bottom in each column: concentrations of A , B , and C , $\ln(\mu)$ and \mathcal{R} at successive time steps ($t = 10, 20, 30$ and 40) at $Pe = 100$ with $R_c = -2$ (first column), $R_c = 0$ (second column), and $R_c = 2$ (equivalent of the nonreactive case, third column). Other parameter values are as in Fig. 4.

the present simulations [5,21,26,44,47–49]. For species A , for instance, we have thus

$$L_a = x|_{(a)=\epsilon} - x|_{(a)=1-\epsilon}. \quad (20)$$

Similarly, the mixing lengths L_b and L_c for the solution of reactant B and the product C , respectively, are defined as

$$L_b = x|_{(b)=1-\epsilon} - x|_{(b)=\epsilon} \quad \text{and} \quad L_c = x|_{(c)>\epsilon}. \quad (21)$$

In the initial diffusive regime, the mixing length varies as $\sim\sqrt{t}$ while it starts to grow faster when the dynamics enters the nonlinear convective regime [50].

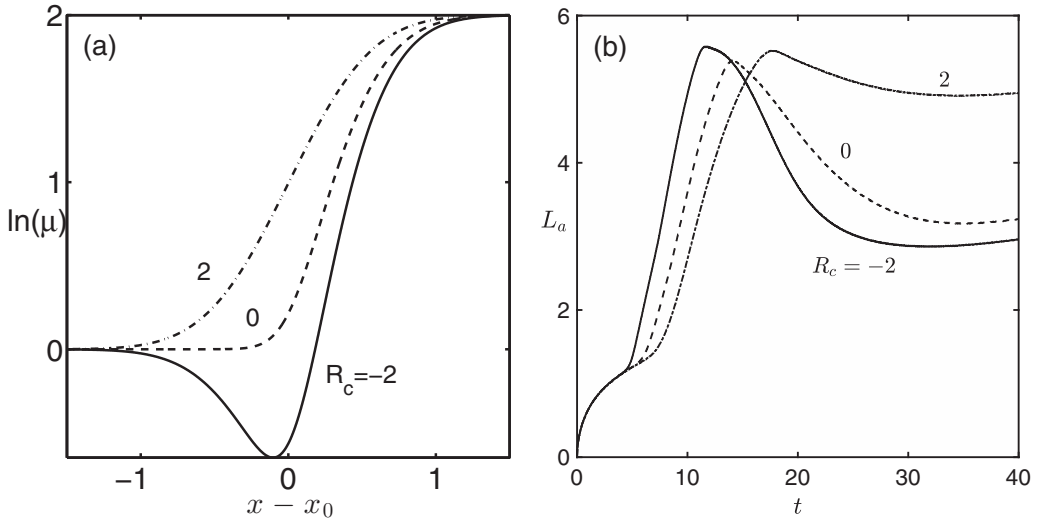


FIG. 8. (a) Long time asymptotic one-dimensional reaction diffusion profiles for $\ln(\mu)$ and (b) temporal variation of the mixing length for A for R_c : -2 (solid line), 0 (dashed line), and 2 (dash-dotted line). Other parameter values are as in Fig. 7.

A. Effect of mobility ratio R_c at $R_b > 0$

The effect of changing the log-mobility ratio R_c is shown in Fig. 7 for three values $R_c = -2, 0, 2$. We remind that, when $R_b = R_c (= 2$ here), the consumption of B is balanced by the production of C ; hence the dynamics of the reactive case is equivalent to that of the nonreactive system. When $0 < R_c < R_b$, the viscosity decreases by the reaction but the viscosity profile remains monotonic in space. On the contrary, if $R_c < 0$, a minimum in viscosity develops in time. For $R_b = 2$, the cases

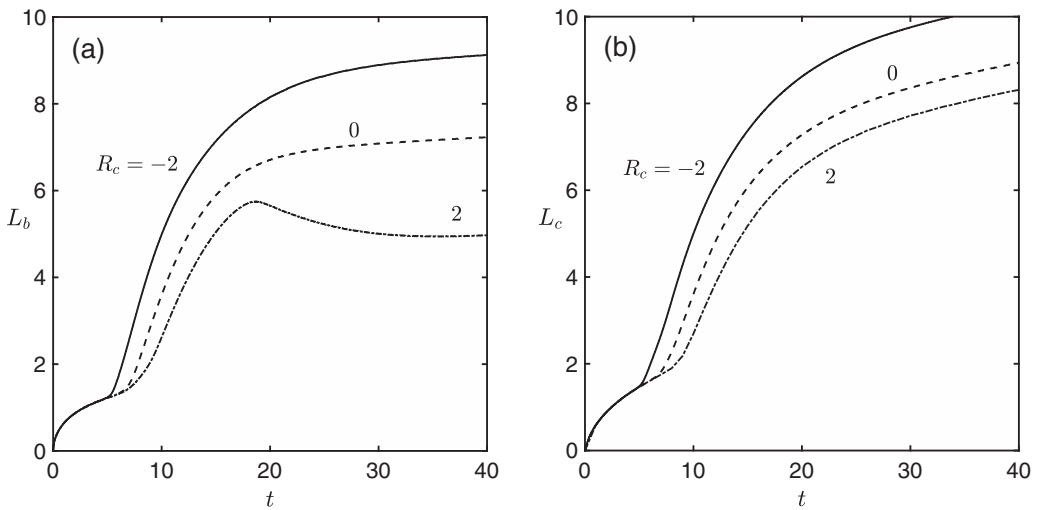


FIG. 9. Temporal variation of the mixing length at R_c : -2 (solid line), 0 (dashed line), and 2 (dash-dotted line) for species (a) B and (b) C . Other parameter values are as in Fig. 7.

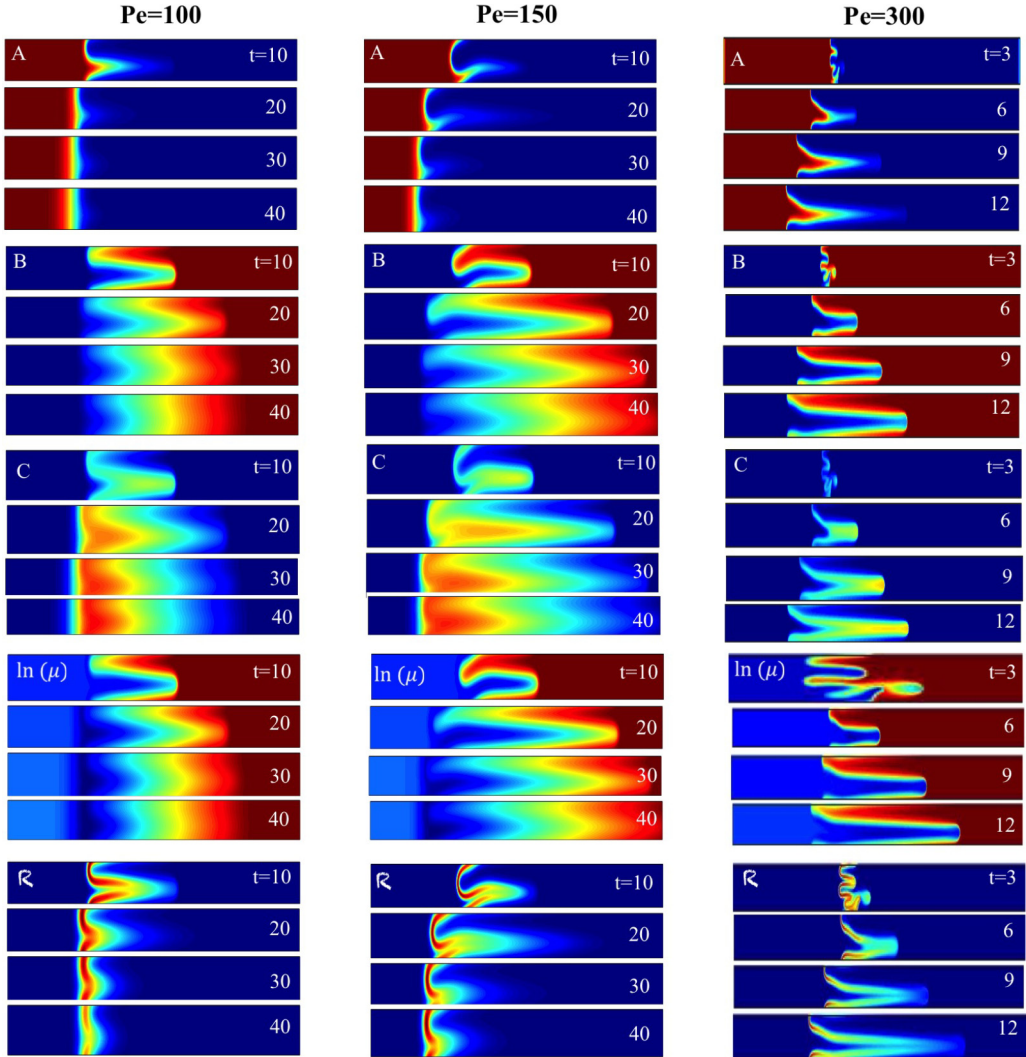


FIG. 10. Same as Fig. 7 but for $R_c = -2$ and different values of Pe: 100 (first column), 150 (second column), and 300 (third column) at different times.

$R_c = 2$, $R_c = 0$, and $R_c = -2$ represent thus the (i) nonreactive VF, (ii) reactive VF with monotonic viscosity, and (iii) reactive VF with a viscosity minimum, respectively.

By comparing concentrations of A , B , and C for various time steps in these three cases, we see that, when $R_c < 0$, the viscosity minimum has the following effects: (i) the interface between A and C stabilizes rapidly and the mixing of reactant A decreases as compared to the other two cases and (ii) as time evolves, the mixing region between C and B increases and stops fingering in time, displacing more B by the product C . The reactive VF is stabilized at low Pe by the viscosity minimum compared to the reactive VF case with monotonic viscosity or the nonreactive VF.

The origin of this stabilization can be explained through the long time asymptotic one-dimensional reaction-diffusion (RD) profiles of $\ln(\mu)$, as shown in Fig. 8(a). If $R_c = -2$, the reaction diffusion viscosity front moves in time from the higher viscosity region of B to the lower viscosity region of A [see Fig. 8(a)]. Due to the presence of a lower viscosity region containing C , the profile of $\ln(\mu)$ develops a minimum in the A -rich region. While the gradients $d(\ln\mu)/dx$ are

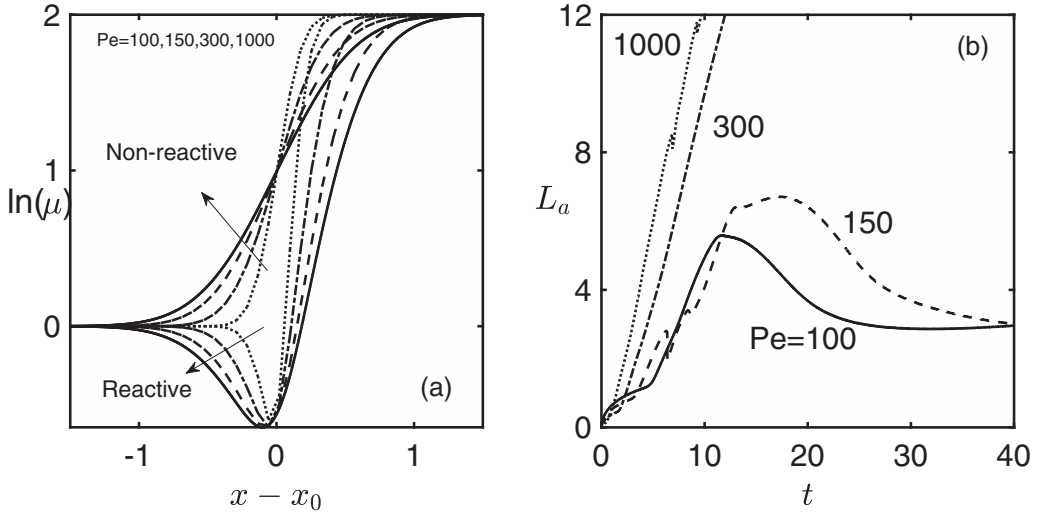


FIG. 11. (a) Long-time asymptotic RD profiles of $\ln(\mu)$ for $Pe = 100$ (solid line), 150 (dashed line), 300 (dash-dotted line), and 1000 (dotted line). Reactive and nonreactive cases are shown by arrows pointing towards curves at decreasing Pe . (b) Temporal evolution of the mixing length of A for different Pe . Other parameter values are as in Fig. 10.

decreasing with R_c on the left of the reaction front ($x - x_0 < 0$), those on the right ($x - x_0 > 0$) are increasing. Specifically, when $x - x_0 > 0$, the slope of the RD profiles of $\ln(\mu)$ becomes steep, steeper, and steepest when R_c takes values 2, 0, and -2 , respectively. On the other hand, when $x - x_0 < 0$ the opposite trend is observed; i.e., the slope tends to the low, lower, and lowest value when R_c is equal to 2, 0, and -2 , respectively. Consequently, in the RDC system, the instability at the interface between A and C (C and B) is suppressed (enhanced) when $R_c = -2$, as observed in Fig. 7. Owing to this, when $R_c = -2$, the miscible interface between A and C is more stable as is the case when a higher viscosity fluid displaces a lower viscosity one. As a consequence, the mixing

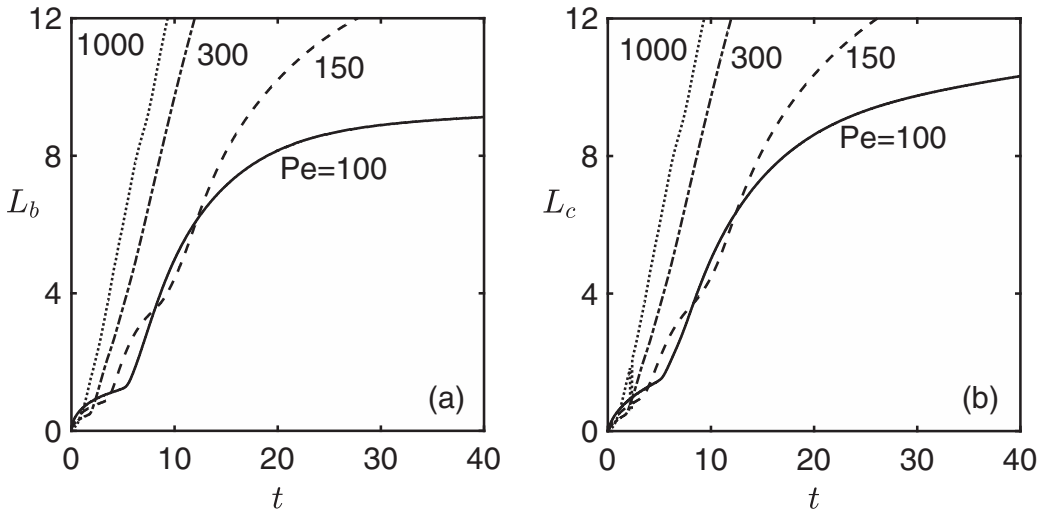


FIG. 12. Same as Fig. 11(b) but for the (a) reactant B and (b) product C.

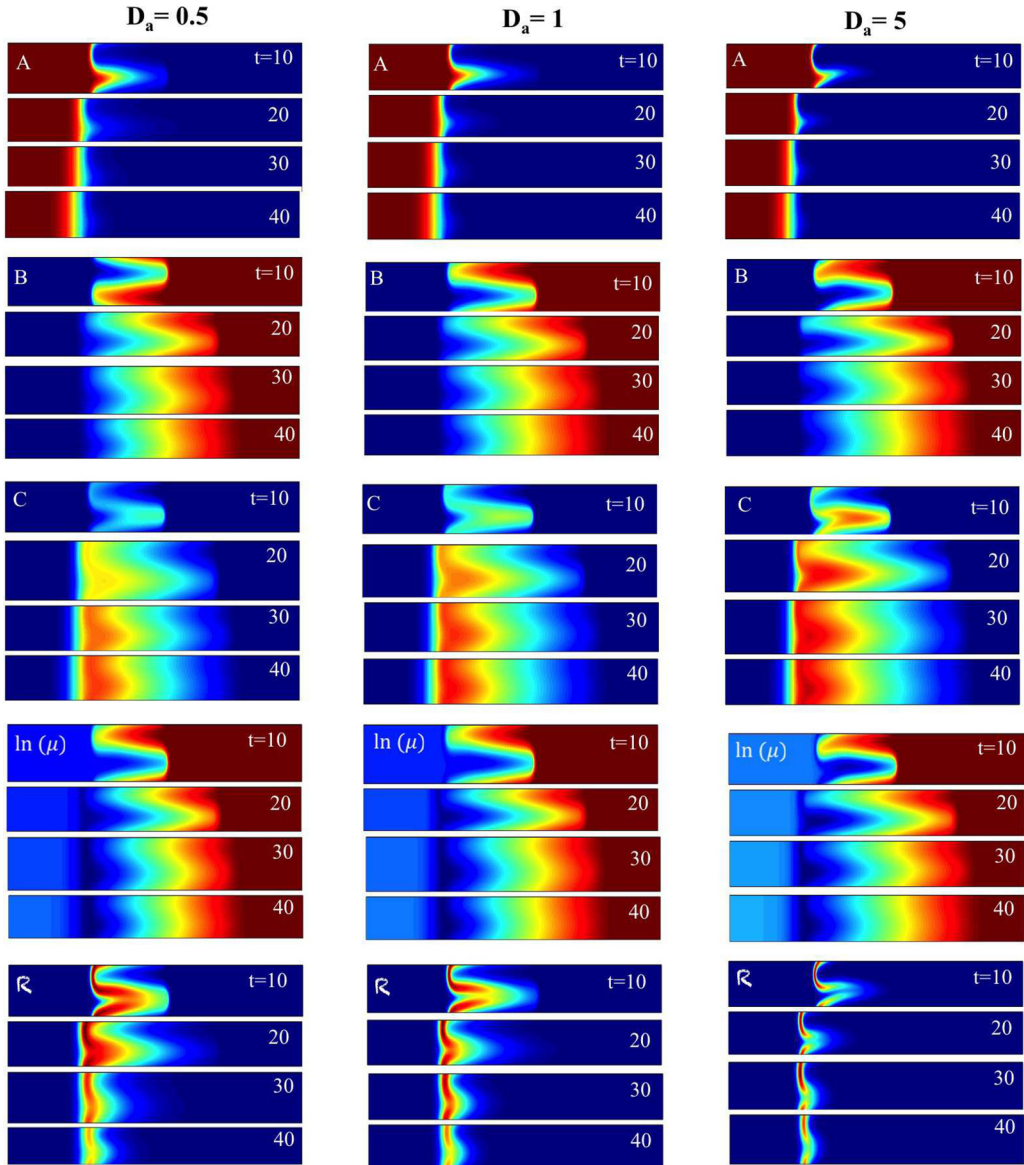


FIG. 13. Same as Fig. 7 but for $Pe = 100$ and different values of D_a : 0.5 (first column), 1 (second column), and 5 (third column).

length L_a of A decreases rapidly as time evolves and finally reaches a steady value which is the lowest among all cases, as shown in Fig. 8(b).

In contrast to the interface between A and C , the interface between C and B is more unstable when $R_c = -2$ because $d(\ln\mu)/dx$ is then the steepest [see Fig. 8(a)]. This can also be noticed in the evolution of the mixing length of B and C in Figs. 9(a) and 9(b). We see from Figs. 9(a) and 9(b) that the mixing between the reactant B and the product C increases more rapidly as R_c decreases. Consequently, the instability at the miscible interface between B and C starts earlier and the mixing lengths L_b and L_c increase more in time as R_c decreases. As time evolves (far from the onset), due to the transverse diffusion, L_b and L_c saturate to a value which increases with decreasing

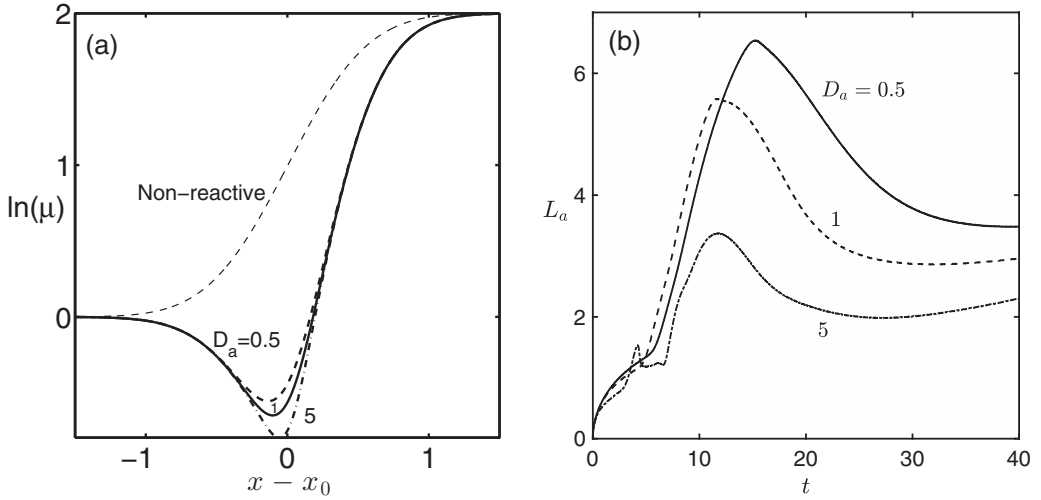


FIG. 14. Same as Fig. 11 for variable Da : 0.5 (thick dashed line), 1.0 (thick solid line), and 5.0 (thick dot-dashed line). The thin dashed line in (a) represents the nonreactive case.

R_c . The widening of the zone rich in B is thus larger when $R_c = -2$ in comparison to $R_c = 0$ and $R_c = 2$ (nonreactive). Thus, the effect of the presence of a viscosity minimum for $R_c < 0$ is that (i) L_a decreases after some time, and (ii) L_b and L_c are larger than in the monotonic ($R_c = 0$) and nonreactive ($R_b = R_c$) cases. From Figs. 4–9, we can thus conclude that, when $R_c = -2$, the front between A and C stabilizes, the mixing between B and C is increased, and the displacement of B is larger.

B. Effect of Péclet number, Pe

In the previous section, we saw in Figs. 8 and 9 that the onset time of fingering (defined as the time at which the mixing lengths depart from the \sqrt{t} diffusive trend) decreases; i.e., the

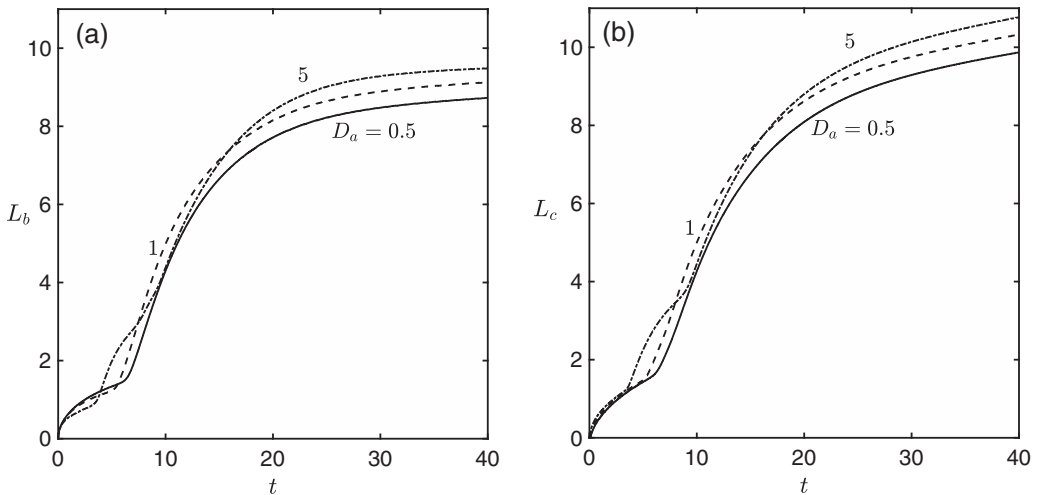


FIG. 15. Same as Fig. 14(b) but for the mixing length of reactant B and product C .

system is initially more unstable as R_c decreases. We now fix $R_c = -2$ and analyze the effect on fingering of changing Pe , keeping it nevertheless at a small value as this is the range where chemical reactions have a stabilizing effect and as the large Pe case has already been partially studied [24]. Specifically, concentrations, log-viscosity, and the reaction rate are shown for $Pe = 100$ (first column), 150 (second column), and 300 (third column) in Fig. 10. We see that the system becomes more unstable when increasing Pe . This can be understood by inspecting the long-time asymptotic one-dimensional RD profiles shown in Fig. 11(a). The nonreactive displacement is more unstable when Pe increases because the gradient of viscosity, $d(\ln\mu)/dx$, is correspondingly sharper. Similarly, viscosity gradients in the reactive RD systems are larger when Pe increases as diffusion is then less efficient to smooth the viscosity profile. Consequently, the RDC system also becomes more unstable with increasing Pe , as shown in Fig. 10, and on the evolution of the mixing lengths [see Figs. 11(b) and 12], where we see that the onset time of the fingering instability decreases with increasing Pe . The smaller Pe , the quicker the mixing lengths tend to a steady state value at low Pe , whereas at large Pe the mixing lengths are increasing irrespective of the viscosity minimum at the interface for RD system. These results again show that, in the limit of large Pe , reactive VF is more intense and the reaction tends to destabilize the system while, in the limit of low Pe , reactive VF is softened and tends to stabilize as compared to the nonreactive case.

C. Effect of Damköhler number, Da

To study the effect of varying the Damköhler number on the stabilization of fingering thanks to reactions decreasing the viscosity, Fig. 13 depicts the concentrations, $\ln(\mu)$, and the reaction rate \mathcal{R} at successive times for three values of Da . We see that, when Da increases (i.e., the reaction occurs faster), the viscosity minimum develops more quickly [see also RD profiles of viscosity in Fig. 14(a)], the amount of product C formed at a given time increases, and the reaction rate \mathcal{R} decays faster because the regions that are depleted in A and/or B which have reacted and have been replaced by C become wider. As a consequence, when Da increases, the miscible interface between A and C stabilizes faster and the steady value of L_a decreases [Fig. 14(c)]. In parallel, the interface between B and C becomes uniform in time, and the corresponding values of L_b and L_c saturate (see Fig. 15). The reactive system is thus globally more stable at low Pe when Da is larger.

We conclude thus from this parametric study that the displacement tends to stabilize (destabilize) at lower Pe (high Pe) for $R_c < 0$, and larger Da (smaller Da). The optimal conditions to avoid fingering can thus be achieved when the viscosity is decreasing by a fast chemical reaction provided the Pe number is kept as low as possible to allow the minimum in viscosity to build up.

V. CONCLUSION AND OUTLOOK

We have here analyzed the influence of varying the Pe number on reactive VF driven by a simple $A + B \rightarrow C$ type chemical reaction decreasing the viscosity *in situ*. To do so, we have numerically integrated Darcy's law for the evolution of the flow velocity and RDC equations for the concentrations coupled by a viscosity profile depending dynamically on the concentration of the chemical species. The relative importance of advection and diffusion has been varied by changing the values of the dimensionless parameter Pe . Nonlinear simulations have been performed to characterize the properties of reactive VF when a solution of a reactant A displaces a solution of B to produce the less viscous product C at the miscible reactive interface. At lower Pe , the VF instability is less intense in both reactive and nonreactive cases because the viscosity gradients are smoothed out by diffusion. The reactive VF pattern covers nevertheless a larger area; i.e., it is spatially denser than the nonreactive pattern. These observations are in good agreement with experiments [20,29]. Similarly to the nonreactive case, at higher Pe , VF is enhanced in reactive systems when the viscosity minimum does not have time to build up. Less-dense fingering patterns and more mixing are then observed. In other words, the fingering patterns at high Pe cover a smaller

area than at low Pe . In terms of displacement efficiency, the presence of a viscosity minimum at lower Pe is found to optimize a homogeneous and regular displacement with less convective mixing.

Our study provides a theoretical framework to control VF in many geophysical processes, e.g., reactive pollutant displacement, CO_2 sequestration, and EOR. Recently, it has been shown that fingering instabilities in the application of EOR can be controlled by introducing a viscosity minimum in the zone of contact between the two fluids via the formation of foam between the injected gas and displaced oil [9]. In this context, the present study (i) provides a connection between viscosity minimum and stabilization, (ii) introduces a way to control VF by controlling the value of the Péclet number, and (iii) shows that, at low Pe , the reactive VF improves the sweep efficiency in comparison to the nonreactive conditions.

ACKNOWLEDGMENTS

We thank Y. Nagatsu, F. Brau, F. Haudin, and M. Mishra for fruitful discussions. P.S. acknowledges IIT Madras for a New Faculty Seed Grant (Grant No. MAT/16–17/671/NFSC/PRIY). A.D. acknowledges FRS-FNRS under the PDR CONTROL grant for financial support.

-
- [1] P. G. Saffman and G. I. Taylor, The penetration of a fluid into a porous medium or Hele-Shaw cell containing a more viscous liquid, *Proc. R. Soc. London A* **245**, 312 (1958).
 - [2] P. G. Saffman, Viscous fingering in Hele-Shaw cells, *J. Fluid Mech.* **173**, 73 (1986).
 - [3] C. T. Tan and G. M. Homsy, Stability of miscible displacements in porous media: Rectilinear flow, *Phys. Fluids* **29**, 3549 (1986).
 - [4] G. M. Homsy, Viscous fingering in porous media, *Annu. Rev. Fluid Mech.* **19**, 271 (1987).
 - [5] C. T. Tan and G. M. Homsy, Simulation of nonlinear viscous fingering in miscible displacement, *Phys. Fluids* **31**, 1330 (1988).
 - [6] F. M. Orr and J. J. Taber, Use of carbon dioxide in enhanced oil recovery, *Science* **224**, 563 (1984).
 - [7] S. R. D. Lunn and B. H. Kueper, Manipulation of density and viscosity for the optimization of DNAPL recovery by alcohol flooding, *J. Contam. Hydrol.* **38**, 427 (1999).
 - [8] X. Fu, L. Cueto-Felgueroso, and R. Juanes, Pattern formation and coarsening dynamics in three-dimensional convective mixing in porous media, *Philos. Trans. R. Soc. A* **371**, 20120355 (2013).
 - [9] R. Farajzadeh, A. A. Eftekhari, H. Hajibeygi, S. Kahrobaei, J. M. van der Meer, S. Vincent-Bonnieu, and W. R. Rossen, Simulation of instabilities and fingering in surfactant alternating gas (SAG) foam enhanced oil recovery, *J. Nat. Gas Sci. Eng.* **34**, 1191 (2016).
 - [10] C. J. Ritsema, L. W. Dekker, J. L. Nieber, and T. S. Steenhuis, Modeling and field evidence of finger formation and finger recurrence in a water repellent sandy soil, *Water Resour. Res.* **34**, 555 (1998).
 - [11] V. Hornof and F. U. Baig, Influence of interfacial reaction and mobility ratio on the displacement in a Hele-Shaw cell, *Exp. Fluids* **18**, 448 (1995).
 - [12] M. Jahoda and V. Hornof, Concentration profiles of reactant in a viscous finger formed during the interfacially reactive immiscible displacements in porous media, *Powder Technol.* **110**, 253 (2000).
 - [13] Y. Nagatsu and T. Ueda, Effects of reactant concentrations on reactive miscible viscous fingering, *AIChE J.* **47**, 1711 (2001).
 - [14] Y. Nagatsu and T. Ueda, Effects of finger-growth velocity on reactive miscible viscous fingering, *AIChE J.* **49**, 789 (2003).
 - [15] Y. Nagatsu, T. Ogawa, Y. Kato, and Y. Tada, Investigation of reacting flow fields in miscible viscous fingering by a novel experimental method, *AIChE J.* **55**, 563 (2009).
 - [16] A. De Wit and G. M. Homsy, Viscous fingering in reaction-diffusion systems, *J. Chem. Phys.* **110**, 8663 (1999).
 - [17] A. De Wit and G. M. Homsy, Nonlinear interactions of chemical reactions and viscous fingering in porous media, *Phys. Fluids* **11**, 949 (1999).

- [18] J. Fernandez and G. M. Homsy, Viscous fingering with chemical reaction: Effect of *in-situ* production of surfactants, *J. Fluid Mech.* **480**, 267 (2003).
- [19] T. Podgorski, M. C. Sostarecz, S. Zorman, and A. Belmonte, Fingering instabilities of a reactive micellar interface, *Phys. Rev. E* **76**, 016202 (2007).
- [20] Y. Nagatsu, K. Matsuda, Y. Kato, and Y. Tada, Experimental study on miscible viscous fingering involving viscosity changes induced by variations in chemical species concentrations due to chemical reactions, *J. Fluid Mech.* **571**, 475 (2007).
- [21] T. Gérard and A. De Wit, Miscible viscous fingering induced by a simple $A + B \rightarrow C$ chemical reaction, *Phys. Rev. E* **79**, 016308 (2009).
- [22] Y. Nagatsu, Y. Kondo, Y. Kato, and Y. Tada, Effects of moderate Damköhler number on miscible viscous fingering involving viscosity decrease due to a chemical reaction, *J. Fluid Mech.* **625**, 97 (2009).
- [23] S. H. Hejazi, P. M. J. Trevelyan, J. Azaiez, and A. De Wit, Viscous fingering of a miscible reactive $A + B \rightarrow C$ interface: A linear stability analysis, *J. Fluid Mech.* **652**, 501 (2010).
- [24] S. H. Hejazi and J. Azaiez, Non-linear interactions of dynamic interfaces in porous media, *Chem. Eng. Sci.* **65**, 938 (2010).
- [25] S. H. Hejazi and J. Azaiez, Hydrodynamic instability in the transport of miscible reactive slices through porous media, *Phys. Rev. E* **81**, 056321 (2010).
- [26] Y. Nagatsu and A. De Wit, Viscous fingering of a miscible reactive $A + B \rightarrow C$ interface for an infinitely fast chemical reaction: Nonlinear simulations, *Phys. Fluids* **23**, 043103 (2011).
- [27] Y. Nagatsu, Y. Kondo, Y. Kato, and Y. Tada, Miscible viscous fingering involving viscosity increase by a chemical reaction with moderate Damköhler number, *Phys. Fluids* **23**, 014109 (2011).
- [28] L. A. Riolfó, Y. Nagatsu, S. Iwata, R. Maes, P. M. J. Trevelyan, and A. De Wit, Experimental evidence of reaction-driven miscible viscous fingering, *Phys. Rev. E* **85**, 015304(R) (2012).
- [29] L. Riolfó, Fingering instabilities in reactive and non ideal systems: An experimental approach, Ph.D. thesis, Université libre de Bruxelles, Brussels, 2013.
- [30] H. Alhumade and J. Azaiez, Stability analysis of reversible reactive flow displacements in porous media, *Chem. Eng. Sci.* **101**, 46 (2013).
- [31] Y. Nagatsu, C. Iguchi, K. Matsuda, Y. Kato, and Y. Tada, Miscible viscous fingering involving viscosity changes of the displacing fluid by chemical reactions, *Phys. Fluids* **22**, 024101 (2010).
- [32] P. H. Bunton, M. P. Tullier, E. Meiburg, and J. A. Pojman, The effect of a crosslinking chemical reaction on pattern formation in viscous fingering of miscible fluids in a Hele-Shaw cell, *Chaos* **27**, 104614 (2017).
- [33] S. Stewart, D. Marin, M. Tullier, J. Pojman, E. Meiburg, and P. Bunton, Stabilization of miscible viscous fingering by a step growth polymerization reaction, *Exp. Fluids* **59**, 114 (2018).
- [34] V. Sharma, S. Pramanik, C.-Y. Chen, and M. Mishra, A numerical study on reaction-induced radial fingering instability, *J. Fluid Mech.* **862**, 624 (2019).
- [35] Y. Nagatsu, Viscous fingering phenomena with chemical reactions, *Curr. Phys. Chem.* **5**, 52 (2015).
- [36] A. De Wit, Chemo-hydrodynamic patterns in porous media, *Philos. Trans. R. Soc. A* **374**, 20150419 (2016).
- [37] A. De Wit, Chemo-hydrodynamic patterns and instabilities, *Annu. Rev. Fluid Mech.* **52**, 531 (2020).
- [38] Y. Nagatsu and T. Masumo (private communication).
- [39] S. Pramanik and M. Mishra, Effect of Péclet number on miscible rectilinear displacement in a Hele-Shaw cell, *Phys. Rev. E* **91**, 033006 (2015).
- [40] T. E. Videbæk and S. R. Nagel, Diffusion-driven transition between two regimes of viscous fingering, *Phys. Rev. Fluids* **4**, 033902 (2019).
- [41] M. Mishra, M. Martin, and A. De Wit, Miscible viscous fingering with linear adsorption on the porous matrix, *Phys. Fluids* **19**, 073101 (2007).
- [42] M. Martin and G. Guiochon, Theoretical study of the gradient elution profiles obtained with syringe-type pumps in liquid chromatography, *J. Chromatogr. A* **151**, 267 (1978).
- [43] L. R. Snyder and J. J. Kirkland, *Introduction to Modern Liquid Chromatography* (Wiley, New York, 1979), pp. 836–839.
- [44] P. Shukla and A. De Wit, Fingering dynamics driven by a precipitation reaction: Nonlinear simulations, *Phys. Rev. E* **93**, 023103 (2016).

- [45] M. Mishra, P. M. J. Trevelyan, C. Almarcha, and A. De Wit, Influence of Double Diffusive Effects on Miscible Viscous Fingering, [Phys. Rev. Lett. **105**, 204501 \(2010\)](#).
- [46] B. Fornberg, *A Practical Guide to Pseudospectral Methods*, Cambridge Monographs on Applied and Computational Mathematics (Cambridge University Press, Cambridge, UK, 1998).
- [47] W. B. Zimmerman and G. M. Homsy, Viscous fingering in miscible displacements: Unification of effects of viscosity contrast, anisotropic dispersion, and velocity dependence of dispersion on nonlinear finger propagation, [Phys. Fluids A **4**, 2348 \(1992\)](#).
- [48] W. B. Zimmerman and G. M. Homsy, Three-dimensional viscous fingering: A numerical study, [Phys. Fluids A **4**, 1901 \(1992\)](#).
- [49] M. Mishra, M. Martin, and A. De Wit, Differences in miscible viscous fingering of finite width slices with positive or negative log-mobility ratio, [Phys. Rev. E **78**, 066306 \(2008\)](#).
- [50] R. A. Wooding, Growth of fingers at an unstable diffusing interface in a porous medium or Hele-Shaw cell, [J. Fluid Mech. **39**, 477 \(1969\)](#).